Proceedings World Geothermal Congress 2020+1
Reykjavik, Iceland, April - October 2021

Designed 3D Seismic Imaging to Better Understand Geothermal Faulted Reservoir, an Upper Rhine Graben Case History

Helene Toubiana[(1)], Nicolas Salaun[(1)], Jean-Baptiste Mitschler[(1)], Guillaume Gigou[(1)], Xavier Carriere[(1)], Alexandre Richard[(2)], Vincent Maurer[(2)]

(1) CGG - 27 avenue Carnot, 91300 Massy Cedex

(2) ES-Géothermie, 5 rue de Lisbonne, 67300, Schiltigheim

helene.toubiana@cgg.com

Keywords: 3D seismic processing, velocity model building, seismic imaging

ABSTRACT

Over the past 35 years, geothermal projects have been developed in the Upper Rhine Graben (URG) to exploit deep geothermal energy. Below a couple of kilometers of sediment, the deep target consists of granitic basement that is highly fractured and hydrothermally altered, which has high reservoir potential. Despite dense 2D seismic coverage, designed for oil exploration (target between 300 and 700 ms), the faults at the top of the granitic basement (between 1400 and 4000 ms) are poorly imaged and their locations remain uncertain. In order to better understand large scale faulting and to ensure viability of future geothermal projects, a 3D seismic survey has been acquired in the French part of the URG during the summer of 2018. This first 3D survey in France specifically for geothermal energy was positioned to cover the sites of the two operational geothermal plants of Soultz-sous-Forêts and Rittershoffen, where several deep wells penetrate the URG basin and its fractured crystalline basement. To maximize the wave penetration and the good imaging of the deep faulting, a low frequency source sweep was used (2 Hz to 96 Hz) with a regular shooting (40 m) and recording (80 m) along source and receiver lines (SLI 320 m, RLI 200 m), leading to a natural bin size of 10 m by 20 m. This paper will describe how the most recent seismic imaging sequence is designed in order to first process the acquired data and then build a depth velocity model allowing for accurate positioning of the faulting. As part of the processing, well control and reservoir information are incorporated to guarantee a proper well tie of the final image and reliable AVO attributes. These attributes will be used for further quantitative reservoir analyses such as fracture and permeability, critical for geothermal system development.

1. INTRODUCTION

The Upper Rhine Graben (URG), with its deep-seated fault systems, is well known for its high geothermal potential (Dornstadter et al., 1999, Kreuter et al., 2003). This area is characterized by several local thermal anomalies associated to the hydrothermal convective cells circulating inside a nearly vertical fracture network in the granite basement and in the Triassic fractured sediments above it (Pribnow and Clauser, 2000; Schellschmidt and Clauser, 1996). Many geothermal projects are operational in the URG, including Landau, Insheim and Bruchsal in Germany, and Soultz-sous-Forêts and Rittershoffen in France (Vidal and Genter, 2018). Moreover, there are new geothermal projects in the exploration phase of deep drilling in the Strasbourg area (Boissavy et al, 2019). The geothermal targets are primarily the granitic basement and its sedimentary cover represented by Permo-Triassic sandstones, both being highly fractured. Generally highly dipping normal faults related to the URG tectonic history are bearing geothermal brines which are exploited for producing electricity like at Soultz or to heat at high temperatures like in the Rittershoffen (Baujard et al., 2018). To better understand the fluid migration and heat transport, and then to further develop geothermal activity, it is key to properly model the connected fractures and faults. Sausse et al. (2007) shows the high value of using seismic imaging to get a proper understanding of the deep underground structure in the case of the URG geothermal project. The available 2D seismic data, for this region, however, has been acquired many years ago for oil and gas prospection (Durst, 1991) and are not well suited for geothermal exploration since they have very few emitted low frequencies (sweep starting from 10 Hz). Moreover, most of these seismic acquisitions are 2D lines and due to the strong complexity of the fault network in the URG, Eichkitz et al., (2009) have shown the importance of using 3D seismic data to increase the reliability of the model.

To better understand faults and fractures present in the deep granite basement, a dedicated 3D wide azimuth seismic survey was acquired by Électricité de Strasbourg in 2018.This survey was designed for geothermal objectives (Richard et al., 2019) using a sweep starting with a very low frequency (2 Hz to 96 Hz) to better penetrate granite basements. The grid bin size was relatively small to better image fault planes and wide azimuth to image deep and complex structures with various ray-paths. As well as the acquisition, the seismic data processing and imaging are also conducted in order to highlight these deep faulted structures while ensuring high resolution in shallower parts of the section.

Despite numerous 2D seismic lines present in the French URG, this was the first 3D seismic data acquired and processed with a geothermal target in France. A repeated processing flow was used, adding an extra processing step each time and checking the 3D migration results. This allows for early delivery of migrated volumes to interpreters and guides the processing sequence. It also provides more confidence that the chosen parameters will benefit the final image and allows the interpreters to closely follow imaging advancements. These close interactions between geologists and geophysicist teams were very beneficial for the final velocity model building.

This paper details the processing sequence put in place in order to better image various geothermal targets present in the region.

2. ACQUISITION AND FIRST QUALITY CONTROL

The 2018-acquisition campaign covered 180 km^2 of the Northern Alsace (Figure 1) and has been acquired on an orthogonal grid leading to a natural bin size of 10 m x 20 m. This broadband 3D seismic survey is the second largest acquired in Metropolitan France. As it was acquired during the harvesting season, it was crucial to minimize the crew movement. For such, a shot blending scheme was implemented to speed up the acquisition and to optimize the productivity. Also, to facilitate the layout of the sensors on the ground, it was chosen to use a bunched string of 6 Geophones SG-10 rather than a receiver array. All these elements led to a higher level of noise (as less onfield-filtering) that the processing had to handle to recover the full value of this modern acquisition. Deblending and merging of seismic data and geometry was done by the field crew and then sent to the imaging center for the next imaging steps.

Once received in-house, the 44,000 shot points were first Quality Controlled (QC) using outlier detection. RMS maps for all shots were created as multi-variant Gaussian distributions and the probability of 'normality' was set depending of the centre of this Gaussian. With such a technique, spiky traces are removed and, more interestingly, singular noise can be spotted and then addressed with a dedicated process. The use of this automatic QC allows the integrity of each shot to be concluded before starting any further processing step. Geometrical issues due to device miss-positioning or badly merged geometry could also be detected.

As the French side of the URG is only covered by a few 2D seismic campaigns (acquired in 1975 and 1985), little information was available in terms of velocity or statics fields. In order to perform preliminary stacks for a more extensive QC, a 1D-velocity law was provided by the field crew.

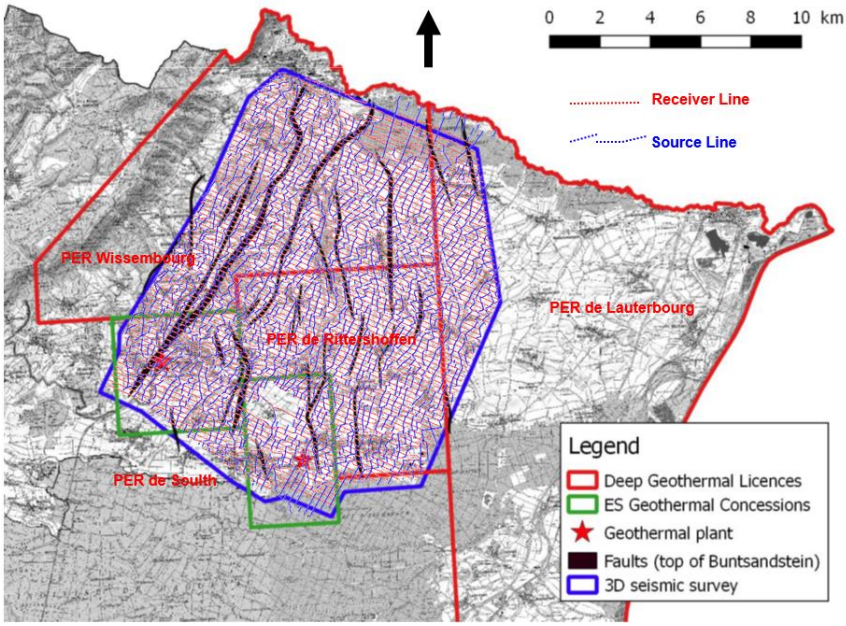

Figure 1: Map of the 2018 180 km^2 acquired 3D Seismic location in French Northern Alsace

3. TIME PRE-PROCESSING

3.1 Statics correction

For a land seismic survey the topography introduces two effects: the first one is the elevation variation between acquisition devices and the second one is the low-velocity geological layers located close to the surface, known as weathering zones (WZ), which are irregular in both thickness and velocity. It is considered that the weathering zone stops when it reaches a consolidated geological layer, which is continuous for the full area. The maximum depth of the WZ varies depending on the region and in this survey it varies from 10 m to 40 m.

Strong local travel-time variations for each source and receiver introduce distortion effects, which need to be compensated to properly recover the seismic reflectors. The common way to compensate for this effect is to apply time static corrections (constant with depth) to move the acquisition devices to a virtual known datum with a known velocity medium. To calculate these static corrections, a model of the weathered layers is computed. On this survey, this model was built using two campaigns of seismic refraction and Up-holes. By interpreting refraction first arrival and calibrating them with drilled Up-holes, we can produce a multi-layer model varying in both velocity and thickness (Figure2c, 2d). This model contains a first layer with very low velocities (250 to 750 m.s^{-1}) and a second layer characterized by velocities between 1050 to 1900 m.s^{-1}. This model, smoothly varying both in thickness and velocity, will explain the low frequency distortion implied by the shallow surface, called primary static correction. An additional correction explaining high frequency variation will then be necessary during the processing sequence, called residual static correction.

Surface consistent static shift corrections are derived from this model and applied for each source and receiver location. After its application, strong geological reflectors are more continuous and overall stacked energy is enhanced (Figure2a, 2b). This step is

critical prior to any velocity analysis as it may help to compensate for the shallow effect. Attenuation of organized noise, such as surface waves, will also suffer from an uncorrected WZ as it will distort noise as well as signal.

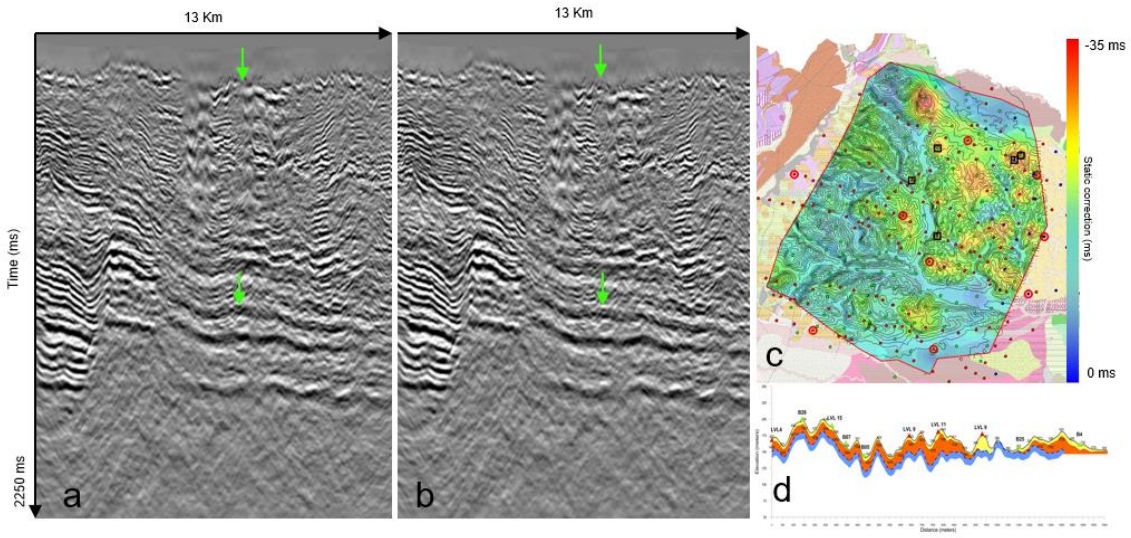

Figure 2: Panels (a) and (b) show stacked seismic sections before and after time static corrections. Green arrows show good geology simplification indicating proper correction for shallow anomaly. Map (c) shows the statics correction value for each surface location. These time corrections are calculated from the derived shallow geological model, example cross-section shown in (d).

3.2 Surface Waves Elimination

The SG-10 geophones used during the acquisition are sensors that need low frequency compensation. This process boosts low frequencies that have been recorded in the field, however, it also boosts the low frequency noise. Being able to properly remove the low frequency noise without damaging the primary signal is key to obtaining a final proper deep section image.

A large part of the emitted energy travels as surface waves, having both longitudinal and/or transverse motion. These waves are the result of interfering P and SV waves that travel along/near the ground surface. They can be decomposed into guided waves and ground roll and are recorded as "pseudo-Raleigh" waves on the geophone vertical component. This large amount of energy needs to be removed at an early stage of the processing in order to better recover the weaker reflected P wave energy. As these waves arrive directly from the source, they are linear at the receiver line in 2D/3D but appear hyperbolic on the broadside receiver lines. Surface waves travel with low velocity, which implies, that with our recording geometry design, most of this energy is heavily aliased. As previously discussed in a primary static section, shallow geological layers are unconsolidated leading to a very slow velocity for the propagation of the surface waves (down to 250 $m.s^{-1}$ on this survey). In order to be able to better model this noise, our first step will be to densely (down to 2.5 m) interpolate our data using a joint low-rank and sparse inversion (Sternfels et al. 2016) to efficiently de-alias these surface waves. Figure 3 (panel b) shows a dense cross-spread after the interpolation that de-aliases the surface waves. The surface waves' velocities vary over the survey location and are also dispersive, requiring different velocities for each frequency.

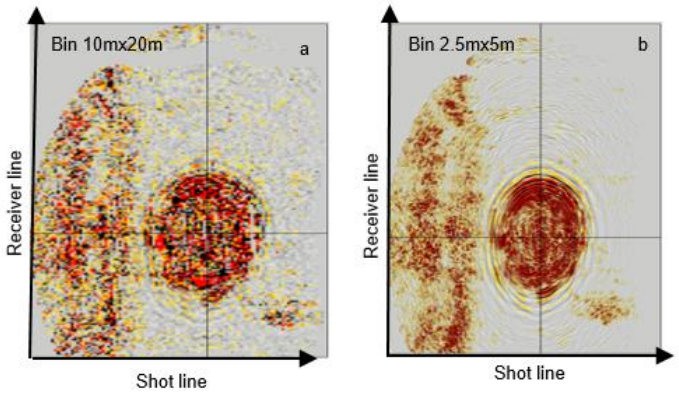

Figure 3: Panel (a) shows a time slice cutting through a cross-spread. Ground roll noise is well visible but are not continuous due to the aliasing which makes it difficult to model. After the densification, panel (b), aliasing is removed and events are easier to follow.

Having our well-sampled data, it is then possible to model these surface waves prior to removal via an adaptive subtraction, which aims to compensate for kinematic inaccuracies in the model. An additional challenge during processing was the poor filtering of the surface waves by the acquisition devices. Land surveys are typically designed to attenuate surface waves traveling transversally and to enhance reflection waves traveling vertically, by using arrays of sources and receivers, each containing several sources and receivers, which are stacked to give a point source and a point receiver. However, as discussed above, in this survey the geophone arrays have been bunched (gathered at the same location) for operational reasons, leading to some areas of poor signal to noise ratio. A complex de-noising method was set up with a data-driven interferometry (Chiffot et al., 2016) that produces a good low frequency model for the ground roll. This model is then adapted in 3D (source, receiver line) in order to improve the separation between noise and primary. Another pass of de-noise is done which aims to account for the strong variability of the surface wave property with the shot and receiver location. An adapted surface wave attenuation (Le Meur et al., 2010) is then applied on the data as illustrated on figure 4.

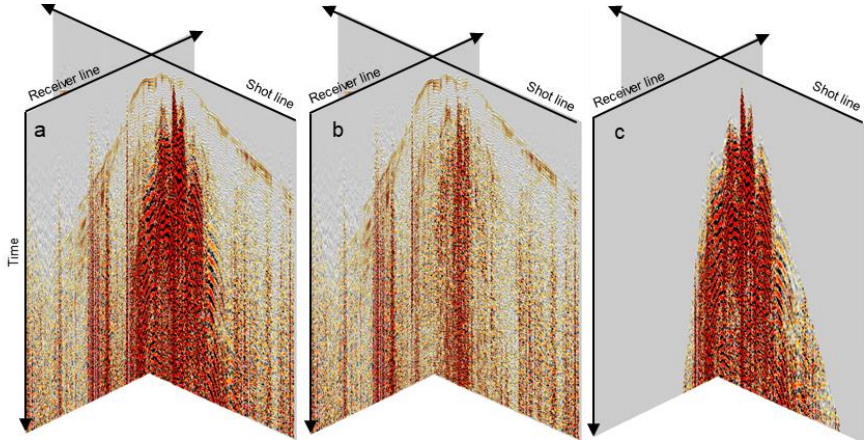

Figure 4: Panel (a) shows a cross-spread (in original geometry) with visible surface waves. Panel (b) is the same cross-spread after the removal of the surface waves and panel (c) illustrates the removed surface waves.

Surface waves can be seen as a cone on shot points that enlarge as the time increases. This means that with our deep faults target, noise coming from surface waves will be spread to a large number of traces and its proper removal is crucial in order to reveal the geology. During this removal, special care was taken to preserve low amplitude primary energy and especially the diffractions, which will image the fault planes.

3.3 Solving shallow heterogeneity via Surface consistent amplitude correction and deconvolution

The French URG 3D seismic acquisition covers an area where the terrain alternates between forest, fields and cities. This large heterogeneity will lead to a various quality of coupling between the acquisition devices and the ground. Coupling quality variation then leads to a different emitted and recorded wavelet magnitude, frequency and phase. To simulate an optimal acquisition and to then link possible variations of the wavelet behavior to deep subsurface rock properties, the surface heterogeneity needs to be corrected. Figures 5a and 5b show a comparison of a dominant frequency map for each shot point and the surface geology. We can observe a high correlation between these two maps, illustrating how soft geological layers will absorb high frequency energy and lead to a low frequency recorded signal.

To correct the wavelet distortion from the near-surface heterogeneities, we used a joint surface-consistent amplitude correction and deconvolution (Garceran & Le Meur, 2012). Computing and applying at the same time the surface consistent amplitude scalars and the surface consistent deconvolution operators via a simultaneous inversion is a consistent way to have a better quality surface with consistent attributes while using the same inversion scheme. During this process, autocorrelation spectra and amplitude scalars are first computed for each trace. We then solve the general surface-consistent equations by performing an inversion on the full survey, estimating the deconvolution operators and then the amplitude scalars. Finally, the surface-consistent deconvolution operators and the surface-consistent amplitude corrections are applied for each survey traces. Figure 5c presents a dominant frequency map after correction where we can see that the survey shallow heterogeneity is reduced. The same QC can be done on the seismic section (Figure 6a, b), where the remaining variation in frequency are now linked to deeper rock properties or imaging quality which will be further assessed in our processing sequence.

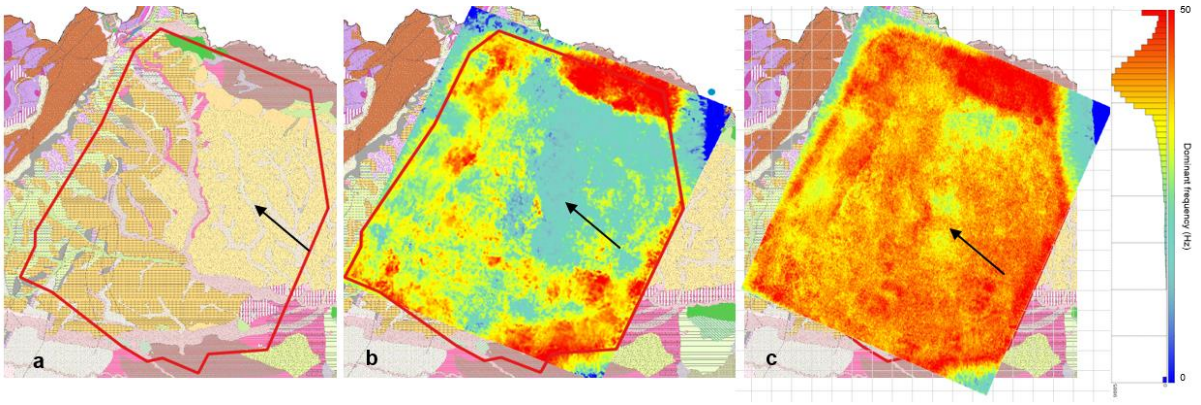

Figure 5: Map (a) shows surface geology which is well correlated with dominant frequency map (b). Absorption can be seen on the center of the survey, illustrated in blue (black arrow). After the application of the surface consistent amplitude correction and the deconvolution, dominant frequency is shifted toward the red, with an average of 35 Hz map (c).

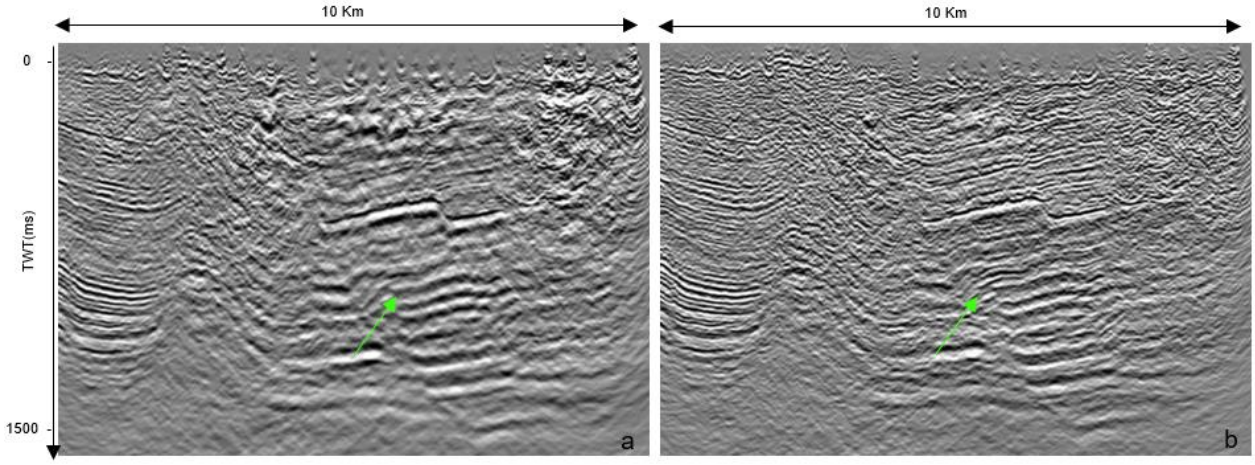

Figure 6: Stacked seismic section before (a) and after (b) surface-consistent amplitude correction and deconvolution. The low frequency area in the middle (green arrows) is compensated leading to more homogeneous frequency content across the section.

3.4 Surface-consistent residual static and velocity update, an iterative process

An accurate P-wave propagation velocity is crucial for the seismic imaging. The velocity contains extensive information about the subsurface properties and is crucial for accurate imaging, which aim to recover earth reflectivity. Usually unknown or only poorly known at a beginning of a seismic exploration project, the velocity field needs to be derived from the data.

Several methods exist to derive velocity from seismic data and this will be further described in the section on depth imaging. At this stage of processing, velocities are used to improve the residual static correction. These two steps are closely linked and it is not a trivial problem to fully decouple velocity and the residual statics, since both have a similar objective metric to reinforce energy of stacked event. It is known that velocity and static corrections can compensate each other. In order to properly separate these two contributions, we chose to iteratively update velocity, then the statics, with freedom constraints and to gradually increase the resolution. In this way, we reduce the risks of over-compensation.

Firstly, an estimation of the RMS velocity derived from the reflected P wave. This estimation is done in the data domain by manually picking the semblance on common mid-point (CMP) gathers. The limit of this method is the strong level of noise present on CMP gathers. To overcome this problem, a velocity update is performed in the image domain by picking on structural stacks. Secondly, once an initial 3D velocity field had been estimated, a pass of residual static correction was carried out. As described in section 3.1, the aim of these corrections is to compensate for the fast variation of the WZ velocity or layer thickness. Due to the impossibility to derive an accurate geological model to better explain the origin of these corrections, a Monte-Carlo scheme was applied (Le Meur, 2011). Constraints for the size of the time shift is set on top of the surface consistent one to avoid compensating for the velocity variation. After the application of this static correction, another iteration of velocity followed by static was carried out, looking for more resolution.

Figures 7a and b illustrate the uplift in reflectivity observed on the stack section. To ensure that faults have not been damaged by wrong static values, QCs have been performed in the pre-stack time migration (PSTM) domain.

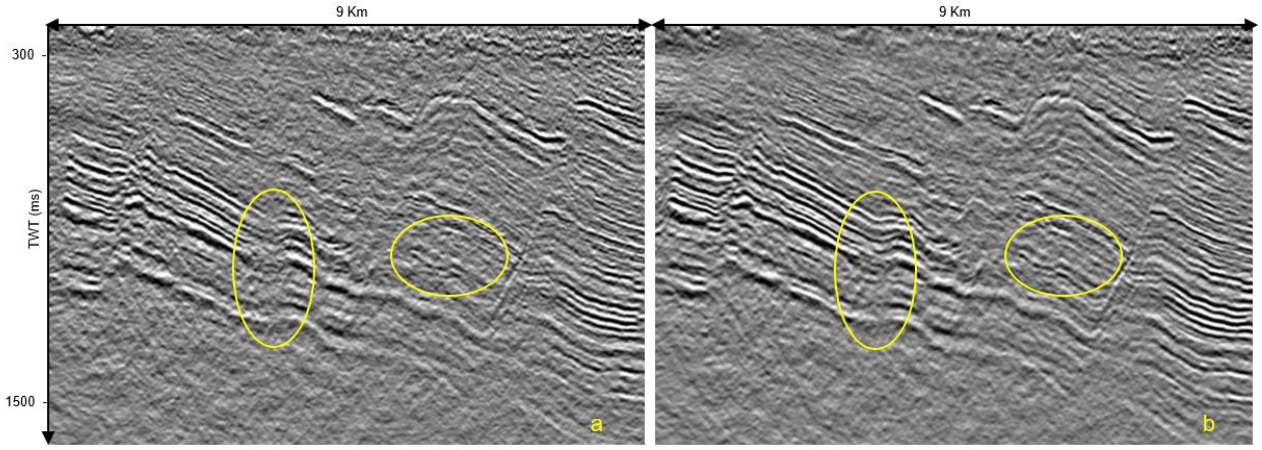

Figure 7: PSTM before (a) and after (b) application of iterative velocity picking and static corrections. On the second panel, a better focusing of the event is well visible helping to better appreciate the reflectivity.

3.5 5D regularization mapping

Migration algorithms rely on the wavefield sampling recorded at the surface by the acquisition devices. When this acquisition is too sparse or irregular it leads to noise and image distortion during the imaging stage. A pass of trace regularization (centering the recorded point at the center of the bin) and interpolation for missing traces is then necessary. During this survey, while the receiver lines were pretty well able to respect the pre-plot design, the shot lines positions were quite irregular due to the terrain (natural obstacles, infrastucture etc.) (Figure 8a). The acquisition set-up had a 200 m spacing between the receiver line and a 320 m spacing between source lines. A 5D interpolation and regularization was used in order to interpolate by a factor of two the source and receiver lines, going from a fold of 150 to a fold of 600.

5D regularization is a global multidimensional interpolator performing simultaneous pre-stack interpolation in five dimensions (offset, azimuth, inline, crossline and time) to predict new shots and receivers at desired locations. During this step, a forward irregular anti-leakage Fourier transform for each dimension is applied on the data followed by a reverse regular Fourier transform back to time-space domain (Poole, 2007). This step also aims to map recorded data to a perfect acquisition geometry (Figure 8b) to reduce possible migration artefacts. Having five dimensions allows better filling of large gaps and ensures homogenized coverage for each offset/azimuth sector, which will be important for subsequent fracture analyzes.

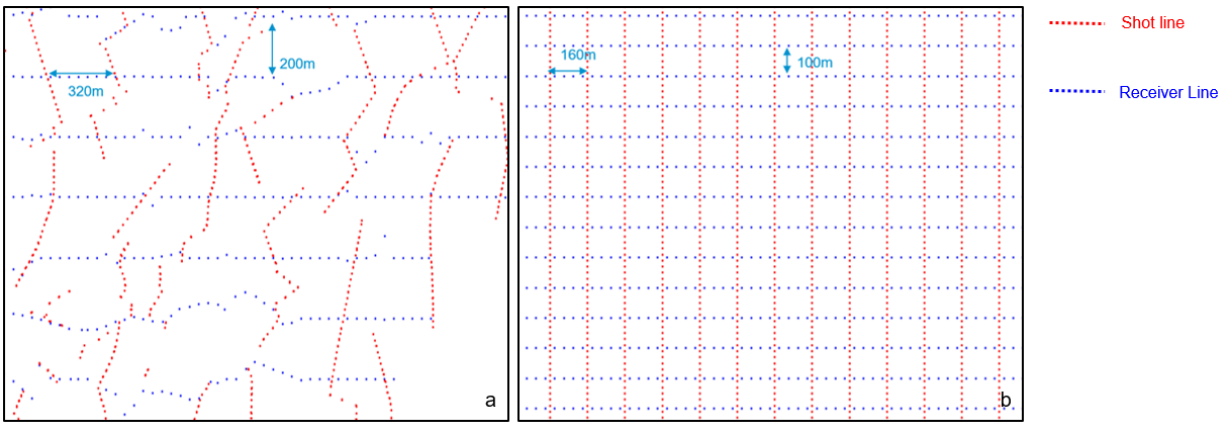

Figure 8: Left map (a) shows actual recorded geometry of the source and receiver line. While the receiver lines (blue) are quite regular, source lines (red) are quite irregular. Data is then mapped to a theoretical perfect acquisition geometry displayed in the right panel (b). Obtained interpolated and densified data will then allow a better sampling of the sub-surface information.

On the seismic data, densification of trace greatly improves the signal to noise ratio (S/N) thanks to fold regularization and it improves the near offsets coverage, and hence the imaging of the near surface (Figure 9).

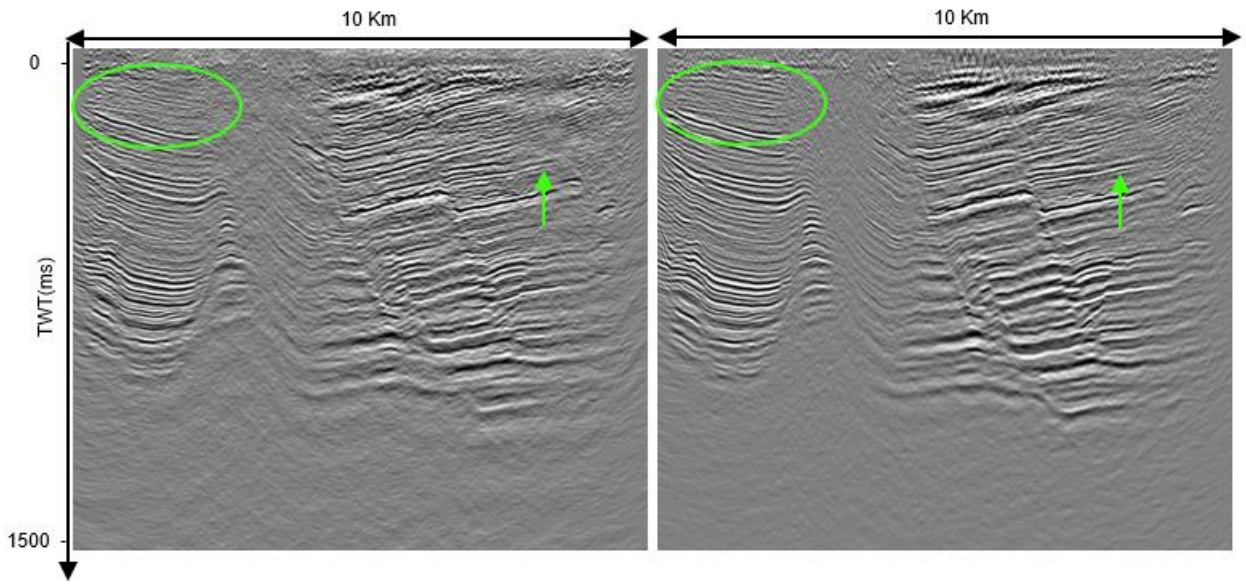

Figure 9: Left PSTM stack section (a) shows a poor shallow surface image and heterogeneity in terms of S/N. After the regularization and the densification (right panel (b)), the S/N is improved (green arrow) making fault plane interpretation easier and the shallow surface is better imaged (green circle).

3.6 Pre-Stack Time Migration

With a regular and densified dataset, we now have access to well-sampled CMPs which will be a great help to further improve the velocity field. At this stage, a non-linear slope time tomography was applied to update migration velocities. This algorithm has the advantage to decouple vertical and horizontal velocity by jointly updating RMS velocity and eta values. The resulting velocity will be close to real geological velocity and should improve the fault imaging.

Time tomography uses the kinematic characteristics of locally coherent events in the un-migrated domain (Depagne et al., 2012). Locally coherent events in a seismic section (position + slopes) are picked in the image domain where the S/N is better. These picks can then be de-migrated to invariants; that is to say the picks of such events in the un-migrated time domain (i.e. independent from the approximations of modeling). Invariants are defined with CMP, offset and time (m, h, T_{obs}) positions & slopes in m and h directions. An invariant can be "kinematically" migrated, it then becomes a facet. Facets correspond to migrated (x, h, T_{mig}) positions and dip in the x and h directions. So facets are equivalent to picks of locally coherent events in the Kirchhoff image (if same travel time modeling in kinematic migration). Dips in the offset direction correspond to the derivative of the residual move-out (*dRMO*). The aim of the time tomography algorithm is to find the velocity model that minimizes *dRMO* what ensures the best flattening of the Kirchhoff time image.

With this new velocity and an ellipticity fields updated, a pre-stack time migration (PSTM) was carried out to obtain our reflectivity. Figure 10 compares the current 3D PSTM with vintage 2D PSTM. While acquisition was quite different with a denser design for 2D and more near offset recording, we can observe that fault imaging has greatly benefitted from the full 3D, full azimuth imaging. The new result also has a much richer low frequency content, that better highlights the thick lithological layers and enhances the fault plane. In the deep part of the section, the Permian (horizon indicated by green arrow) is now better defined and easier to track. The network of faults present below this event is now visible, which will be of a great use for further geothermal activity developments.

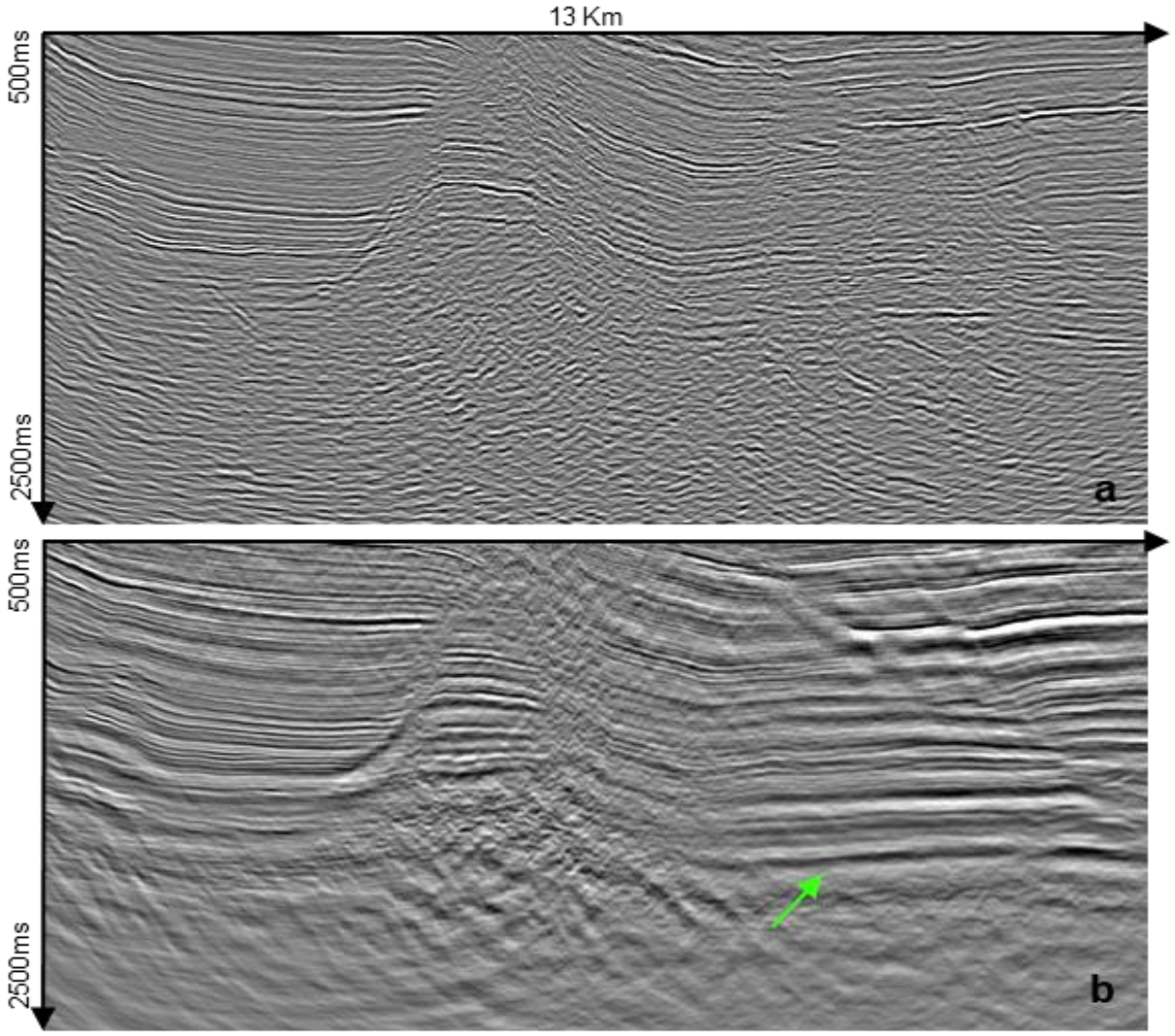

Figure 10: Panel a shows a vintage result coming from the 2D acquisition. A nice resolution can be observed on the shallow part but not on the deeper part of the section. 3D acquisition plus new processing (b) shows a higher resolution in the shallow part and a fully interpretable deep part of the section.

4. DEPTH IMAGING

For complex structures, time imaging suffers from limitations. The principal limitation is the lateral invariance of the velocity. This means that for a CMP location, travel times coming from the source or the receiver will be considered to be traveling with the same velocity. In the case of a strong fault the velocity contrast across the fault cannot be honored, which leads to distortion in the image. In the URG significant faulting is clearly visible, so proper imaging and deep event positioning is crucial for successful well planning. This part will now further describe the flow applied to derive an accurate depth velocity model.

4.1 First break inversion

As discussed above, a usual approach to get access to velocity information from seismic data is to use the Residual Moveout (RMO) of the CMP. However, for the shallow events, where few traces are recorded, it is not possible to extract RMO curvatures from CMPs. Another way is to use the refracted P-wave energy. Already used for static corrections, this information gives us access to velocities of the shallow layers. After picking the first arrivals for each shot point, these are used in a tomography process in order to estimate a velocity model for the shallow section. When comparing the result with the well sonic log (Figure 11), it is seen that the obtained velocity follows a similar trend. In contrast to the RMS velocity, working with the interval velocity requires first solving the shallow velocity before updating deeper, to avoid compensating for shallow effects. Even if it is not intuitive, this first break inversion is then an important step to ensure final imaging of deep target faults.

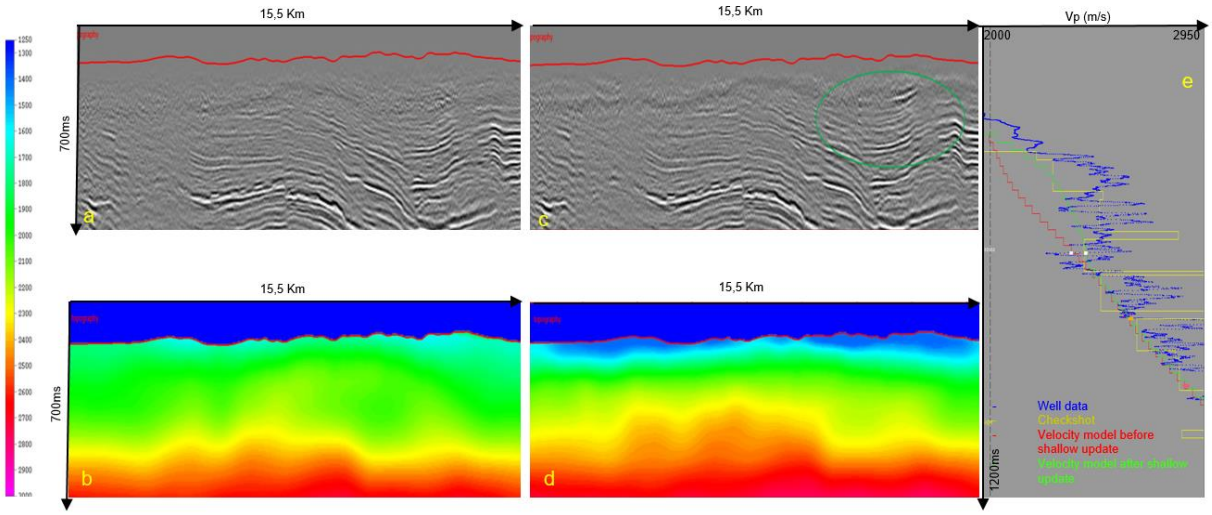

Figure 11: Panel (a) shows a depth migrated shallow part of the section with the initial velocity model (b). After application of the first-break inversion, the velocity now increases in the shallow part (d) improving the seismic event focusing (c). Obtained velocity trend shows a good correlation with the measured check shot (e).

4.2 Multi-layer tomography

As shallow velocity layers have to be found prior to updating deeper ones, velocity model building usually relies on layer-by-layer inversions using a blocky approach. On the other hand, multi-layer tomography (Guillaume et al., 2012) allows for inverting all layers at the same time. The tomographic principle is similar to the one described in section 3.6 but having several layers allows to better constrain each layer and then obtaining a more accurate result. For this purpose, geological horizons need to be interpreted. On this project three horizons were defined as key for the velocity model building as they marked strong velocity contrast, either acceleration or deceleration.

As for the time tomography, depth ML tomography will give us access to velocity, plus delta and epsilon values. Initial models for epsilon and delta have been derived from wells. Nine wells are covering the region and have been extensively analyzed (Vidal et al., 2018). Having access to these wells allowed us to calibrate our velocity and then to obtain a seismic image that matches the depth markers. More horizons where picked for the calibration purpose. Figure 12a shows a tomographic velocity field with horizons overlaid and 12b shows a velocity profile against a recorded sonic log. Strong velocity variations between layers are well captured and follow the sonic velocity profile. Very little mis-tie between the markers and the seismic is visible, indicating that the estimated velocity, in addition to flattening gathers (tomographic constraint), is also accurately located in depth.

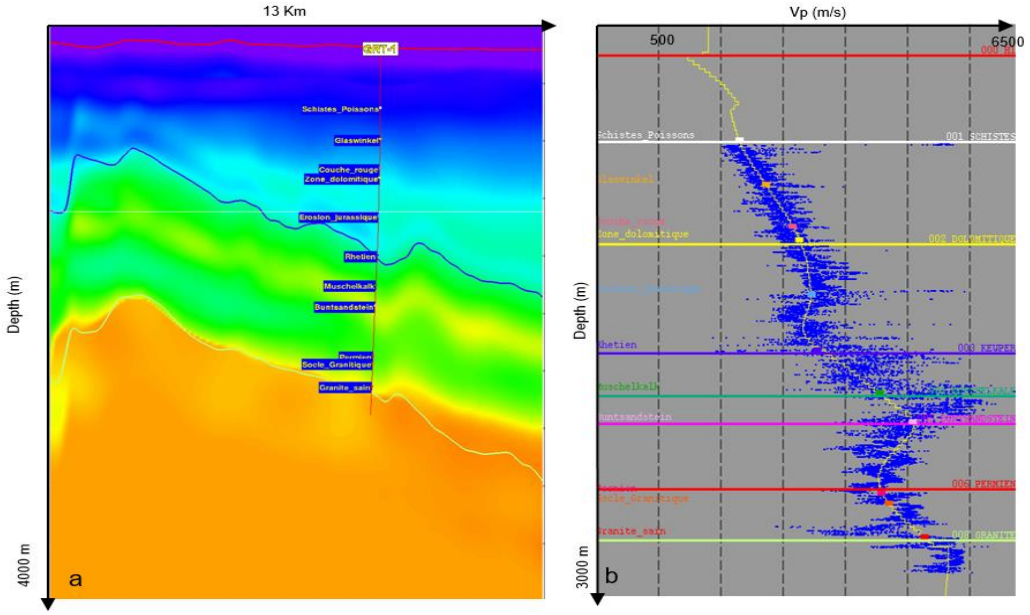

Figure 12: Panel (a) presents the velocity field for one inline overlaid with a picked main horizon. The velocity follows geological details and strong contrasts are observed. These contrasts accurately follow the sonic log (b). This confirms that velocity obtained is actual vertical velocity free of anisotropic effects. The markers in various colors on the well profile confirm the good calibration between the seismic and available well information.

4.3 Fault-constrained tomography

Depth imaging honors fast lateral velocity changes. However, during tomographic inversion, regularization constraints are used to obtain a geological velocity smoothing possible fast-changing velocity artefacts. In the case of sharp faults with a strong throw, leading to a significant velocity variation across the fault, this fast variation will tend to be smoothed leading to incorrect imaging. A fault constraint is then set to limit the regularization constraint in the vicinity of the fault plane. For this purpose, two main fault planes were picked and provided to the tomography, on top of the above-described horizons. Figure 13 shows the velocity field before and after the application of the fault constraint with the corresponding seismic image. Introduction of this contrast in the velocity field for the pre-stack depth migration (PSDM) enables the flattening of events on each side of the fault and a sharper imaging of the fault planes (Figure 14).

For granite basement velocity, scans have been carried out and have been used as well reference velocity information. As wells were mainly drilled for oil exploration purpose only, one well gave us access to the granite basement velocity. Final velocity obtained was then used for the final imaging.

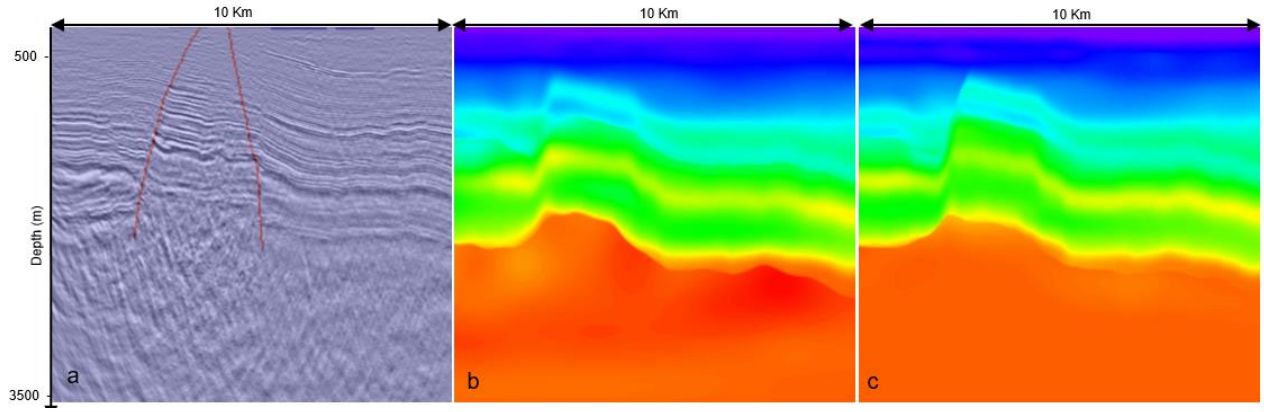

Figure 13: Picked fault planes in red (panel a) are then used in the tomography to obtain a sharp velocity contrast (c). This result could be compared to the classical tomography result where the fault flank is slightly blurry (b).

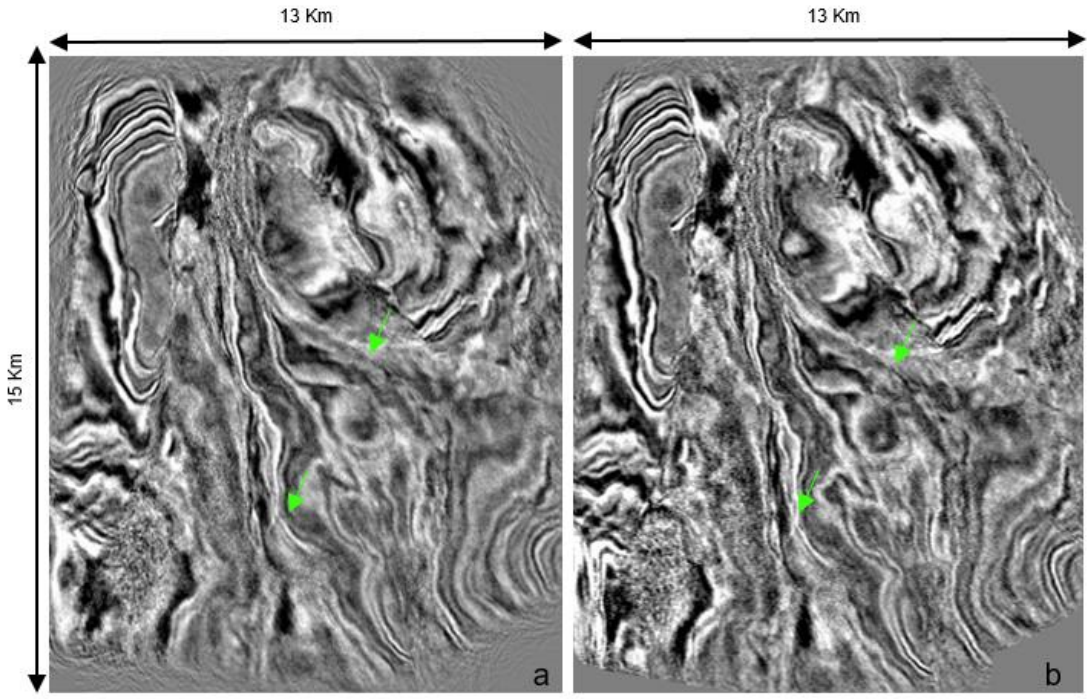

Figure 14: Final PSTM with the Time-tomography (a) vs Final PSDM with the fault-constrained tomography (b). Introduction of the fault constraint allows to better image the fault planes, which are easier to follow along the time slice (at 1sec) as highlighted with green arrows.

5. DISCUSSION

Up until now, large parts of the French URG geological interpretation was performed using the available 2D PSTM data. While valuable for its good shallow resolution, these sections always failed to properly image the top of the altered granite and the fault network present underneath. The goal of this depth imaging project, combined with the optimized time pre-processing, was to

improve the deep imaging, especially the altered granite layer where factures and faults already showed the high geothermal value of this region. The main objective is to better understand the thickness of the layer and how the fault network is organized, in order to better understand the geological history of the deep URG and to further develop geothermal activity.

Having access to 3D data also allows the confirmation and expansion of the interpretation from the shallow part of the 2D data. 2D acquisition design is very effective for good shallow resolution, thanks to full near offset records and regular spatial sampling, while 3D acquisition design is sparse, which may compromise the shallow imaging. It is therefore important to focus not only on the deep part of our 3D survey but also to obtain similar or better results than those available 2D sections for the shallow. With iterative work on the static correction solution, advanced de-noising processes to attenuate the apex of surface waves, effective regularization, and trace densification, we managed to obtain a proper image of the shallow part of the data. With efforts carried out to preserve low frequencies throughout the processing and by deriving an accurate depth velocity model, the obtained result for the deep part of the section is entirely new for interpreters (Figure 15). Steep dips present in the deep part of the section cannot be properly imaged with a 2D line, but need a full 3D wavefield recording and imaging.

It is now possible to interpret and pick 3D horizons for the full area with much more certainty than before. 3D picked and calibrated horizons give a robust starting point before starting the interpretation. To ease interpretation and the picking of the smaller faults, seismic attributes have been extracted from the final volume. Figure 16 illustrates a depth slice coherency map where small and medium size faults are now clearly visible. With full AVO compliant processing and more advanced interpretation, such fracture characterization can be carried out and provide even more information on the French URG geological features.

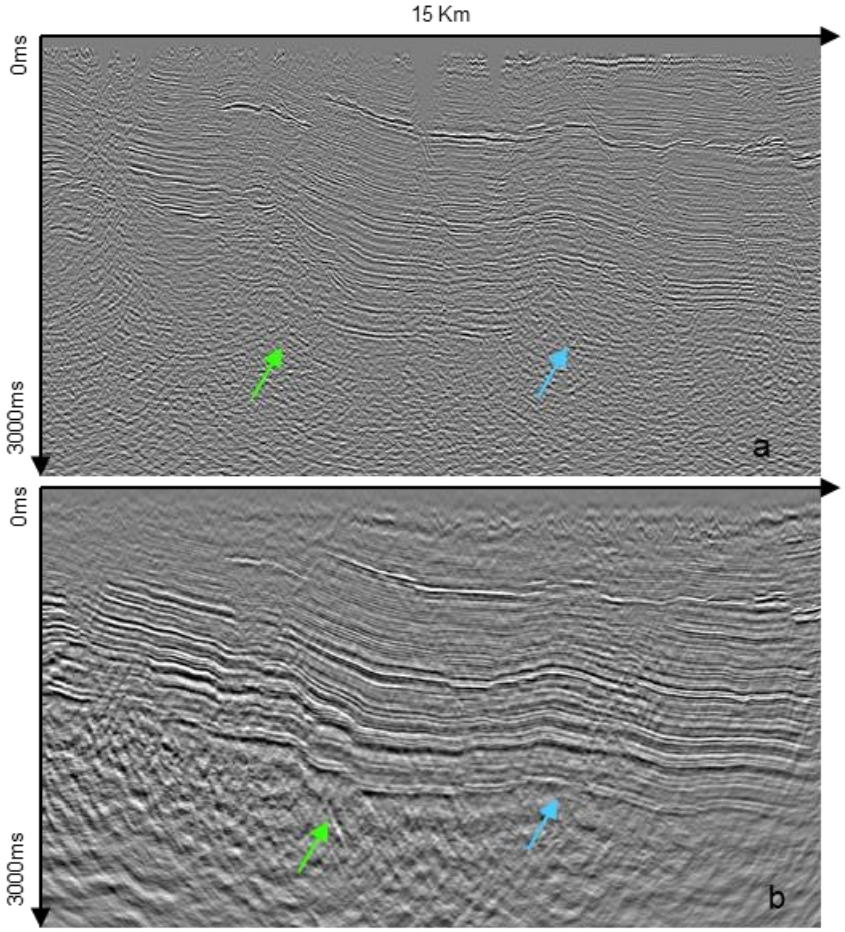

Figure 15: The vintage 2D PSTM (a) is compared to a random line in the new 3D PSDM volume (b). While the shallow part of the data is well defined with the 2D section, greatly benefiting from the acquisition design, the target deep part of the section is fully revealed in the new volume. Top altered granite (blue arrows) is now easy to track on the full survey and the faulted structure present underneath (green arrows) are clearly visible.

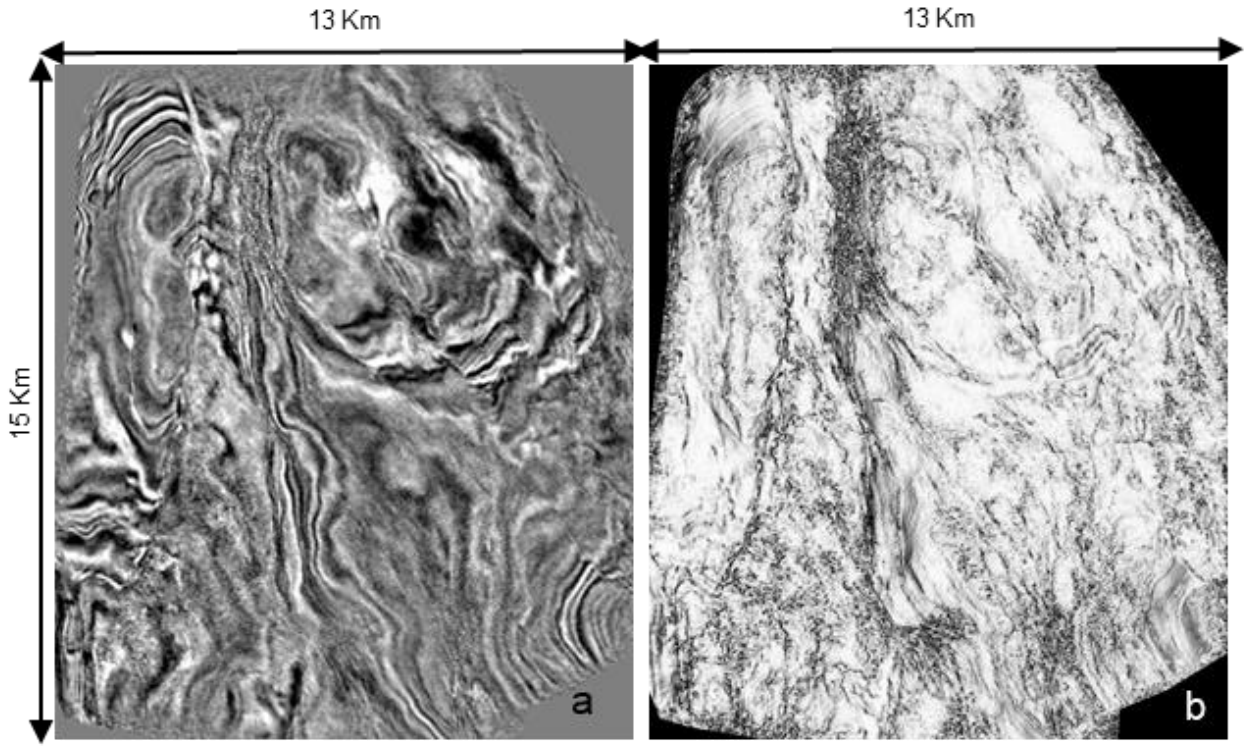

Figure 16: Depth seismic slice (a) is compared with the coherency map (b). The second map highlights the fault continuity which makes it easier to follow and eases the interpretation of this complex fault network.

CONCLUSION

A seismic acquisition campaign was launched in 2018 by Electricité de Strasbourg with the objective to fully image the deep granitic basement and its associated faults. After a complete sequence of the time processing, facing challenges of the low velocity shallow zone and the poor signal to noise area, a depth velocity model was built. For this model, the latest techniques such as first break tomography, multi-layer and fault constraint tomography have been used to deliver a velocity field, maximizing common image gather flatness and minimizing mis-ties with the well. Throughout the processing, several 3D migrations were performed for Quality Control purposes, enabling the client and interpreters to decide what needed to be improved. The repeated processing flow allowed for intermediate data interpretation and ensured the desired quality of the final delivered product. The final volume shows great improvement compared to the 2D vintage PSTM, by accurately imaging the deep part of the URG structure. Possible extraction of attributes such as the coherency map will ease the interpretation of the complex faulted structure. Finally, proper calibration of the delivered seismic image with available wells will be of great value for future location planning.

REFERENCES

Baujard, C., Genter, A., Cuenot, N., Mouchot, J., Maurer, V., Hehn, R., Ravier, G., Seibel, O., Vidal J., (2018). Experience from a successful soft stimulation and operational feedback after 2 years of geothermal power and heat production in Rittershoffen and Soultz-sous-Forêts plants (Alsace, France), Geothermal Resource Council, GRC2018, October 14-17, Reno, Nevada, USA, 2241-2252.

Boissavy, Ch., Henry, L., Genter, A., Pomart, A., Rocher, Ph., Schmidlé-Bloch V., (2019). Geothermal Energy Use, Country Update for France, European Geothermal Congress, EGC 2019, 11-14 June 2019, The Hague, The Netherlands.

Chiffot, C., Prescott, A., Grimshaw, M., Oggioni, F., Kowalczyk-Kedzierska, M., Cooper, S., & Johnston, R. (2017). Data-driven interferometry method to remove spatially aliased and nonlinear surface waves. In SEG Technical Program Expanded Abstracts 2017 (pp. 4980-4985). Society of Exploration Geophysicists.

Depagne, S., Wabara, K., Deladerrire, N., Guillaume, P., Lambar, G., Tour, J. P., & Lafet, Y. (2012). Revealing Velocities-From Time Imaging to High Definition Tomography. In 74th EAGE Conference and Exhibition incorporating EUROPEC 2012. Dornstädter, J., Kappelmeyer, O., & Welter, M. (1999). The geothermal potential in the Upper Rhine Graben valley. In European Geothermal Conference Basel'99. Proceedings (Vol. 2, pp. 77-85).

Durst, H. (1991). Aspects of exploration history and structural style in the Rhine graben area. Generation, accumulation and production of Europe's hydrocarbons. Eur Assoc Petrol Geosci Spec Publ, 1, 247-261.

Eichkitz, C. G., Schreilechner, M. G., Scholz, A., Lotz, U., & Greiner, G. (2009). Upper Rhine Graben–3D Seismic–A New Approach to Geothermal Exploration in a Structurally Complex Tectonic Environment. In 71st EAGE Conference and Exhibition incorporating SPE EUROPEC 2009.

Garceran, K., & Le Meur, D. (2012, June). Simultaneous joint inversion for surface-consistent amplitude and deconvolution. In 74th EAGE Conference and Exhibition incorporating EUROPEC 2012.

Guillaume, P., Hollingworth, S., Zhang, X., Prescott, A., Jupp, R., Lambaré, G., & Pape, O. (2012). Multi-layer tomography and its application for improved depth imaging. In SEG Technical Program Expanded Abstracts 2012 (pp. 1-5). Society of Exploration Geophysicists.

Kreuter, H., Harthill, N., Judt, M., & Lehmann, B. (2003). Geothermal power generation in the Upper Rhine Valley, the project Offenbach/Pfalz. In Proceedings of International Geothermal Conference.

Le Meur, D., Benjamin, N., Twigger, L., Garceran, K., Delmas, L., & Poulain, G. (2010). Adaptive attenuation of surface-wave noise. First Break, 28(9).

Le Meur, D. (2011). Monte-Carlo statics on large 3D wide-azimuth data. In 73rd EAGE Conference and Exhibition incorporating SPE EUROPEC 2011.

Poole, G., & Herrmann, P. (2007). Multidimensional data regularization for modern acquisition geometries. In SEG Technical Program Expanded Abstracts 2007 (pp. 2585-2589). Society of Exploration Geophysicists.

Pribnow, D., & Clauser, C., (2000). Heat and fluid flow at the Soultz Hot Dry Rock system in the Rhine Graben, in: Proceedings of World Geothermal Congress 2000. Kyushu - Tohoku, Japan.

Richard, A., Gillot, E., Maurer, & V., Klee, J. (2019). Northern Alsace (France): the largest geothermal exploration by 3D seismic reflection, European Geothermal Congress, EGC 2019, 11-14 June 2019, The Hague, The Netherlands.

Sausse, J., Dezayes, C., & Genter, A. (2007). From geological interpretation and 3D modelling to the characterization of the deep seated EGS reservoir of Soultz (France). European Geothermal Congress, Unterhaching, Germany, 29 May-01June 2007

Sternfels, R., Prescott, A., Pignot, G., Tian, L., & Le Meur, D. (2016, May). Irregular Spatial Sampling and Rank-reduction-Interpolation by Joint Low-rank and Sparse Inversion. In 78th EAGE Conference and Exhibition 2016.

Vidal, J., & Genter, A. (2018). Overview of naturally permeable fractured reservoirs in the central and southern Upper Rhine Graben: Insights from geothermal wells. Geothermics, 74, 57-73.